Structure and Properties of Regenerated *Antheraea pernyi* Silk Fibroin Filaments

Baoqi Zuo,[1] Leigen Liu,[2] Feng Zhang[1]

[1]*School of Materials Engineering, Soochow University, Suzhou, Jiangsu 215006, People's Republic of China*
[2]*Suzhou Institute of Trade and Commerce, Suzhou, Jiangsu 215021, People's Republic of China*

Received 30 November 2006; accepted 2 March 2009
DOI 10.1002/app.30347
Published online 24 April 2009 in Wiley InterScience (www.interscience.wiley.com).

ABSTRACT: Degummed *Antheraea pernyi* silk fibroin (APSF) fibers were dissolved in a lithium thiocyanate solution that was dialyzed against distilled water for 3 days. Solution-cast APSF films were dissolved in hexafluoroisopropanol to prepare a spinning solution. Wet spinning was employed to prepare APSF filaments. Scanning electron microscopy, X-ray diffraction, Fourier transform infrared spectroscopy, Raman spectroscopy, solid-state ^{13}C cross-polarization/magic angle spinning nuclear magnetic resonance, and differential scanning calorimetry were employed to study the regenerated APSF filaments. The results showed a uniform distribution of molecular weights, and the largest one may have been greater than 200 kDa. The regenerated filaments contained β-sheet, α-helix, and random-coil conformations, and their breaking strength was 52.20% of the breaking strength of the native fibers. © 2009 Wiley Periodicals, Inc. J Appl Polym Sci 113: 2160–2165, 2009

Key words: fibers; FT-IR; NMR; structure; X-ray

INTRODUCTION

In comparison with the amino acid composition of *Bombyx mori* silk fibroin, the amino acid composition of *Antheraea pernyi* silk fibroin (APSF) is characterized by an abundance of alanine (Ala), glycine (Gly), and serine (Ser) and significant amounts of asparagine (Asp) and arginine (Arg). This composition is related to the abundance of —$(Ala)_n$— repeats in the primary structure, which is thought to favor the formation of an α helix, and the presence of the tripeptide sequence Arg–Gly–Asp, which is known to be effective in cell attachment.[1–5] On the basis of these features, there have been several reports on the application of APSF in advanced biomedical areas, such as cell culture substrates and tissue engineering matrices. However, there are few reports concerning regenerated APSF filaments.

APSF solutions can be obtained by two methods. One is to directly disperse into water the liquid silk secreted in the posterior mature silk gland. Magoshi et al.[6] reported that both exothermic and endothermic peaks in differential scanning calorimetry curves of APSF films shifted to higher temperatures with an increasing heating rate. The conformational transition from an α-helix structure to a β-sheet crystalline structure was induced in solution-cast APSF films by a heat treatment above the glass-transition temperature at about 200°C.[7] Tsukada[8] found that the α–β transition depends on the drying rate of the liquid silk fibroin solution as well as the drying temperature. After β transformation, the silk fibroin membranes are no longer water-soluble, and they display superior mechanical properties and thermal stability.[9–11] The other method is to use a chemical solvent to dissolve native degummed APSF fibers, but this method decreases the molecular weight of APSF. Tsukada et al.[12] obtained a regenerated APSF film by dissolving APSF in a lithium thiocyanate solution, and they investigated its physicochemical characteristics and thermal stability. Kweon and coworkers[13,14] prepared a regenerated APSF film by dissolving APSF in a calcium nitrate solution, and they studied the effects of heat and methanol treatments on the structure and molecular conformation of the film.

However, few studies on regenerated APSF filaments have been reported. In this work, a regenerated APSF solution was prepared by the dissolution of waste native degummed APSF fibers in lithium thiocyanate, and regenerated APSF filaments were obtained by wet spinning. The structure and

Correspondence to: B. Zuo (bqzuo@suda.edu.cn).
Contract grant sponsor: Six Talents Peak Project of Jiang Su; contract grant number: [2006]174.
Contract grant sponsor: Natural Science Foundation of Jiang Su; contract grant number: BK2007054.
Contract grant sponsor: National Base Research Program of China (973 Program); contract grant number: 2005CB623906.

TABLE I
Compositions of the 5% Concentrating Gel (3 mL) and 10% Separating Gel (15 mL)

Composition	5% concentrating gel	10% separating gel
Water (mL)	2.1	5.9
30% acrylamide mixture (mL)	0.5	5.0
1 mol/L Tris at pH 6.8 (mL)	0.38	—
1.5 mol/L Tris at pH 8.8 (mL)	—	3.8
10% SDS (mL)	0.03	0.15
10% persulfuric acid (mL)	0.03	0.15
N.N.N.N-Tetramethyle thylenediamine (mL)	0.003	0.009

mechanical properties of the regenerated filaments and native fibers were investigated. The aim of this study was to supply an experimental basis for the application of APSF in biomedical materials.

EXPERIMENTAL

Materials

A. pernyi silk fibers were degummed three times with a 5 g/L Na_2CO_3 aqueous solution at 98–100°C for 30 min and then washed with distilled water. The purified silk fibroin was dissolved in a 16*M* lithium thiocyanate solution (Sigma–Aldrich Co., United States) for 1 h at 50°C. The solution was dialyzed in a cellulose tube (molecular cutoff = 8000–14,000) against water for 3 days. APSF films were obtained through the casting of the aqueous silk fibroin solution onto a polystyrene plate at 20°C and air-dried for 3 days. Then, the APSF films were dissolved in hexafluoroisopropanol (HFIP; Dupont Chemical Solutions Enterprise, Wilmington, United States) for 6 days at 25°C to prepare a wet-spinning solution.

The spinning solution was introduced into a cylinder at room temperature. A pressure of 2.5–4.0 MPa was applied to the spinning dope to extrude it into an anhydrous ethanol coagulation bath with a spinneret with an orifice length of 0.6 mm and an orifice diameter of 0.5 mm. The resulting fibers were drowned and rolled up and then were set in a stream; in this way, the regenerated APSF fibers were obtained.

Methods

The molecular weight of the APSF aqueous solution was measured with a Hoefer Mini VE flat-plate electrophoresis meter (Amersham Pharmacia Biotech, Uppsala, Sweden). Polyacrylamide gel electrophoresis was performed at 20 mA for 30 min first and then at 40 mA. Gels were stained with Coomassie Brilliant Blue R-250. The compositions of the 10% separating gel and 5% concentrating gel are listed in Table I.

The surface morphology of the fibers was observed with scanning electron microscopy (SEM; S-520, Hitachi, Tokyo, Japan) at 20°C and 60% relative humidity. Samples were mounted on a copper plate and sputter-coated with a gold layer 20–30 nm thick before imaging; the diameters of the fibers were acquired from randomly collected SEM images with a Leica (Wetzlar, Germany) BME biomacroscope. For each sample, the diameter was the average of 100 measurements.

X-ray diffraction curves were recorded with a model 2027 diffractometer (Physics Electric Machine Co., Tokyo, Japan) with Cu K radiation from a source operated at 40 kV and 30 mA. The scanning rate was 2°/min, and the diffraction angle (2θ) ranged from 5 to 45°.

Fourier transform infrared (FTIR) spectra were obtained with a Magna (Madison, United States) spectrometer in the spectral region of 400–4000 cm^{-1}.

Raman spectra were obtained with an Olympus BX40 spectrometer (Middlesex, UK) in the spectral region of 800–1700 cm^{-1}.

Solid-state ^{13}C cross-polarization/magic angle spinning nuclear magnetic resonance (NMR) spectra were obtained on a DSX-300 spectrometer (Bruker Co., Karlsruhe, Germany) operating at 75.4 MHz with a cross-polarization contact time of 1 ms, a recycle delay time of 3 s, magic angle spinning at 4 kHz, and a 1H 90° pulse of 4.35 μs.

Differential thermal analysis (DTA) curves were obtained with a PE-SII thermal analysis instrument (Perkin Elrmer, Shizuoka, Japan) at a heating rate of 10°C/min with a nitrogen gas flow rate of 120 mL/min and a scanning temperature range of 20–500°C.

The mechanical properties were measured with an automatic tensile tester (model 3365 electronic strength tester; Instron, Boston, USA) at 20°C and 65% relative humidity. Various parameters were set as follows: sensor range, 50 cN; gripping length, 10 mm; tensile rate, 10 mm/min; force accuracy, 0.01 cN; and elongation accuracy, 0.01 mm.

RESULTS AND DISCUSSION

Electrophoresis of a regenerated *A. pernyi* aqueous solution

Sodium dodecyl sulfate (SDS) was used to analyze the purified and crude sericin (8%), and sodium dodecyl sulfate/polyacrylamide gel electrophoresis (SDS–PAGE) showed a single band; the molecular weight was approximately 200 kDa.[15] Figure 1 shows the results of SDS gel electrophoresis of a regenerated APSF aqueous solution. The electrophoresis pattern showed a continually stained region range of 60.0–200.0 kDa, indicating that the

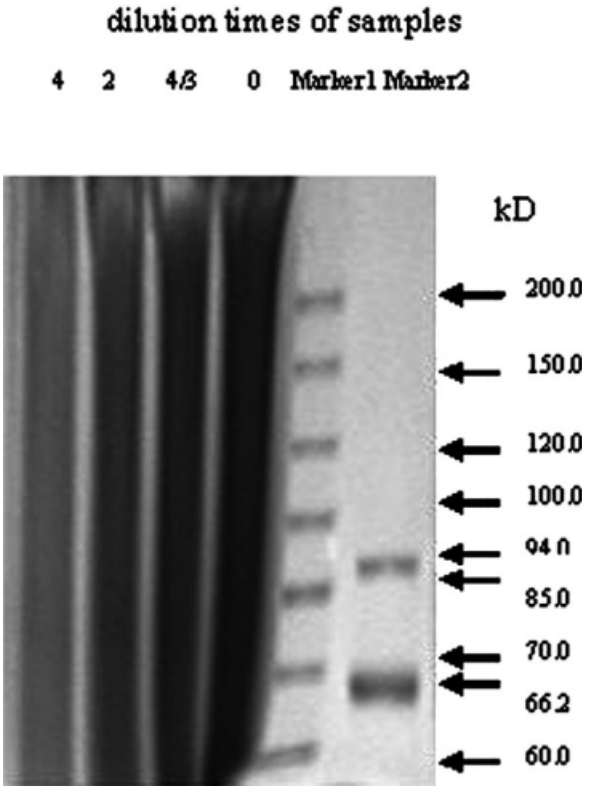

Figure 1 SDS–PAGE patterns of regenerated APSF that was dissolved in 16*M* lithium thiocyanate at 50°C for 1 h.

regenerated silk fibroin was composed of a mixture of polypeptides with a uniform distribution of molecular weights, and the largest one may have been greater than 200 kDa. It has been reported[16] that the molecular weight of APSF collected directly from the posterior division of the silk gland is 400–450 kDa. Therefore, we can assume that the regenerated silk fibroin underwent extensive depolymerization by scission of the main fibroin chains.

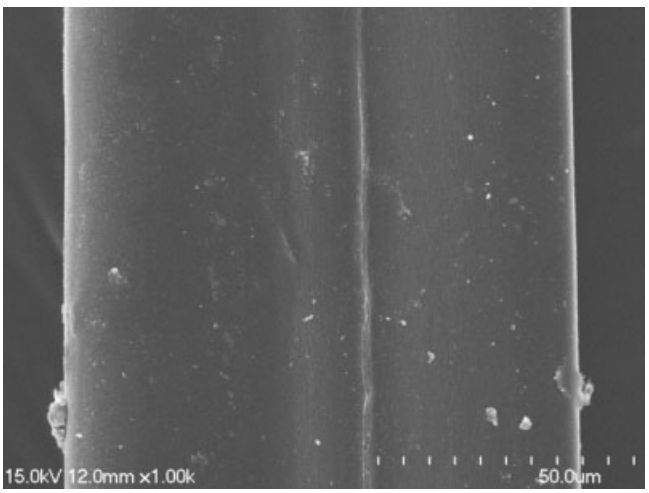

Figure 3 SEM picture of a longitudinal section of regenerated APSF fiber.

SEM microscopy

As shown in Figures 2 and 3, there was no significant difference in the longitudinal surface morphology between the native and regenerated fibers. A comparison of Figures 4 and 5 shows that the cross sections of native fibers were coarser than those of regenerated fibers and had several holes, possibly because of corrosion by the Na_2CO_3 solution during the degumming process. In addition, it looks as if the regenerated filaments had a more condensed structure; maybe this was due to the lower molecular weight of the regenerated fibers and the crystalline process induced by ethanol. The diameters of the native and regenerated fibers were 0.0208 and 0.0369 mm, respectively.

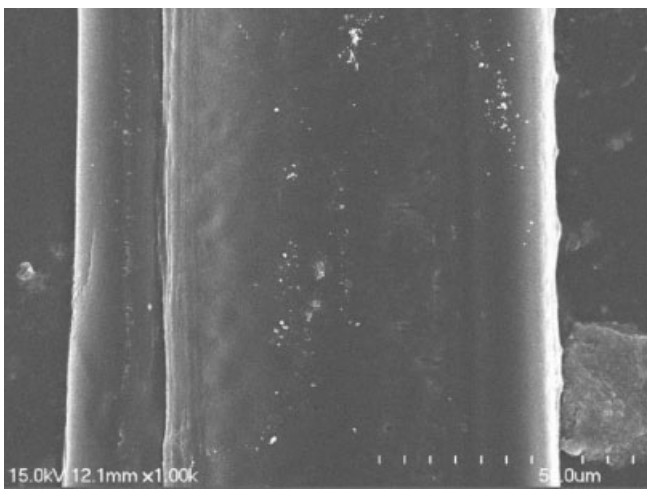

Figure 2 SEM picture of a longitudinal section of native APSF fiber.

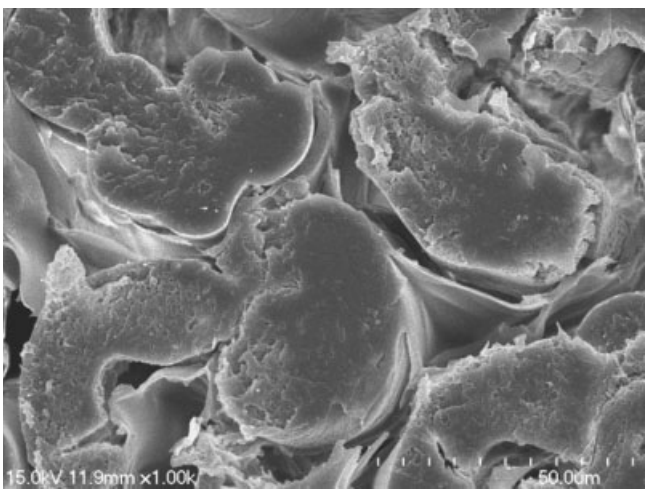

Figure 4 SEM picture of a cross section of native APSF fiber.

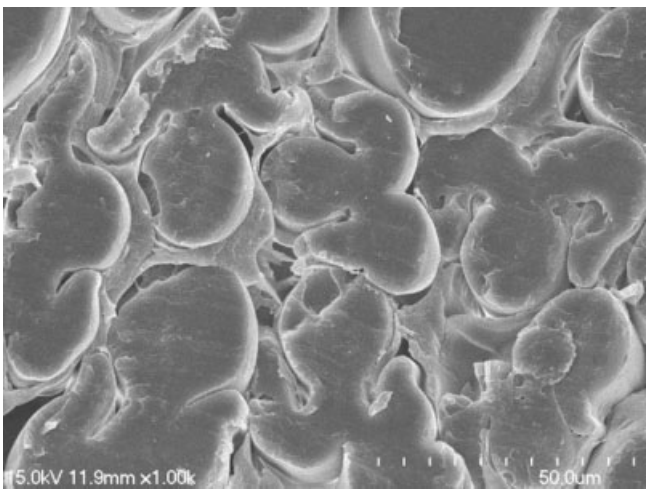

Figure 5 SEM picture of a cross section of regenerated APSF fiber.

X-ray diffraction curves

Figure 6 shows the X-ray diffraction curves of APSF samples. X-ray diffraction patterns of APSF have been provided in earlier reports.[9,13,17,18] According to the results of these reports, the diffraction peaks at 16.4 (lattice spacing $d = 5.40$ Å), 16.8 (5.27 Å), 20.1 (4.41 Å), and 20.3°(4.37 Å) belong to the β-sheet structure, and that at 24.1° (3.69 Å) belongs to the α-helix structure. On the basis of these data, Figure 6 shows that the crystalline component of the native and regenerated APSF filaments mainly consisted of β sheets but had a few α helices. In addition, the diffraction intensity at 16.8° became much weaker after regeneration, and this demonstrated that the regenerated fibers had lower crystallinity than the native silk.

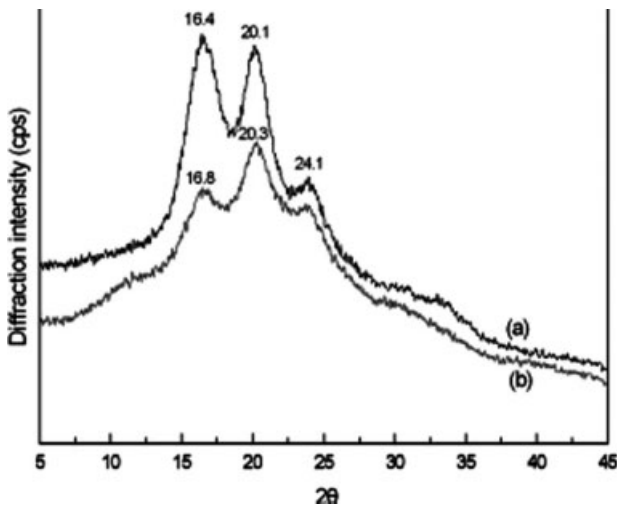

Figure 6 X-ray diffraction curves of (a) native APSF fibers and (b) regenerated fibers.

FTIR spectroscopy

IR spectroscopy is a technique widely used to study the molecular conformation and crystalline structure of silk proteins. The position and intensity of the amide band are sensitive to the fibroin.[19] Figure 7 shows FTIR spectral patterns of *A. pernyi* silk fibers. The pattern of the nature fibers [Fig. 7(a)] shows strong absorption bands at 1515.6 (amide II), 1236.1 (amide III), 964.8 (amide IV), and 699.2 cm^{-1} (amide V) due to the β-sheet structure,[8,13,14,20] and the band at 621.2 cm^{-1} (amide V) can be attributed to the α-helix conformation.[18] On the other hand, the pattern of the regenerated fibers shows strong absorption bands at 1515.4 (amide II), 1237.3 (amide III), and 964.9 cm^{-1} (amide IV) due to the β-sheet structure, and the bands at 1654.6 (amide I), 1541.6 (amide II), and 619.6 cm^{-1} (amide V) can be attributed to the α-helix conformation.

In comparison with the pattern of the native fibers, in the pattern of the regenerated fibers, new absorption bands at 1654.6 (amide I) and 1541.6 cm^{-1} (amide II), attributed to the α-helix conformation, appeared, but absorption bands at 1515.6 (amide II), 1236.1 (amide III), and 699.2 cm^{-1} (amide V), attributed to the β-sheet structure, disappeared. The β-sheet contents in the natural APSF fibers and regenerated APSF filaments were 42.1% and 27.2%, respectively, according to the calculation method described by Tsukada et al.;[21] this indicated that the molecular conformation of the regenerated fibers had changed a lot.

Raman spectroscopy

Raman spectroscopy can help us to examine the molecular conformation of a protein that is not reflected in FTIR spectroscopy. Raman spectra of native and regenerated APSF fibers were measured in the

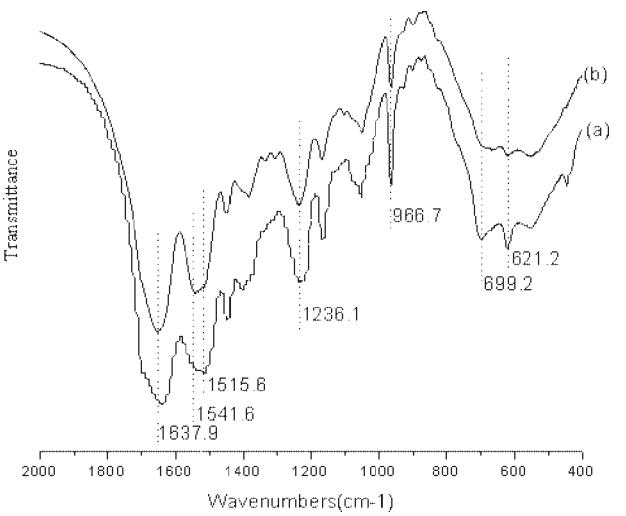

Figure 7 FTIR spectral patterns of (a) native APSF fibers and (b) regenerated fibers.

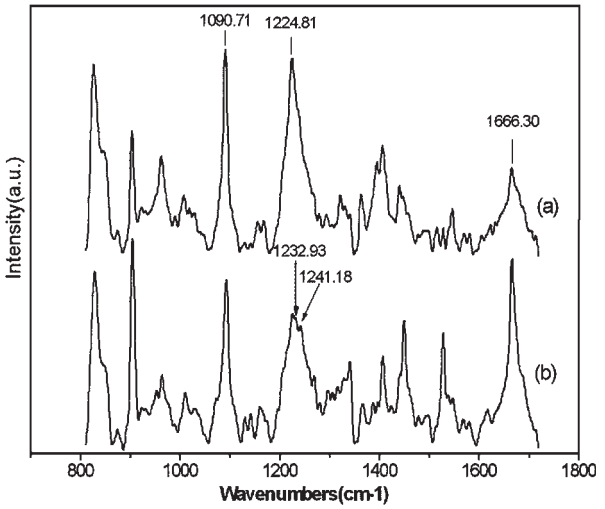

Figure 8 Raman spectral patterns of (a) native APSF fibers and (b) regenerated fibers.

spectral region of 1800–800 cm^{-1}. As shown in Figure 8, the bands of native silk fibroin fibers at 1666.30 (amide I), 1224.81 (amide III), and 1090.71 cm^{-1} were attributed to the β-sheet conformation. Differences in the Raman spectra of the native fibers and regenerated fibers were observed in amide III; a new shoulder peak that appeared at 1241.18 cm^{-1} (amide III) because of splitting of amide III in the antiparallel β-sheet conformation was attributed to the random-coil conformation.[20] On the basis of this analysis and the results of FTIR spectra and X-ray diffraction, it can be suggested that the regenerated fibers contained β-sheet, α-helix, and random-coil conformations.

NMR spectroscopy

The ^{13}C-NMR chemical shifts of carbon atoms in proteins are sensitive to the secondary structure, and this makes ^{13}C-NMR an effective tool for analyzing the secondary structure of silk fibroin. Relationships between conformations and ^{13}C-NMR shifts are well established: the chemical shifts near 17 ppm are attributed to the random-coil conformation; those near 16, 43, 53, and 176 ppm are assigned to the α-helix conformation; and those near 20, 49, 55, 63, and 172 ppm are due to the β-sheet structure.[22,23]

Figures 9 and 10 show ^{13}C cross-polarization/magic angle spinning NMR spectral patterns of native APSF fibers and regenerated fibers, respectively. The native fibers were characterized by the presence of four resonance peaks: Ala C_β at 20.489 ppm and Ala C_α at 48.915 ppm, Ser C_α at 54.668 ppm and Ser C_β at 63.812 ppm, and Ala C=O at 172.171 ppm (all attributed to the β-sheet structure) and Gly C_α at 42.573 ppm (attributed to the α-helix conformation). In comparison with the native fibers,

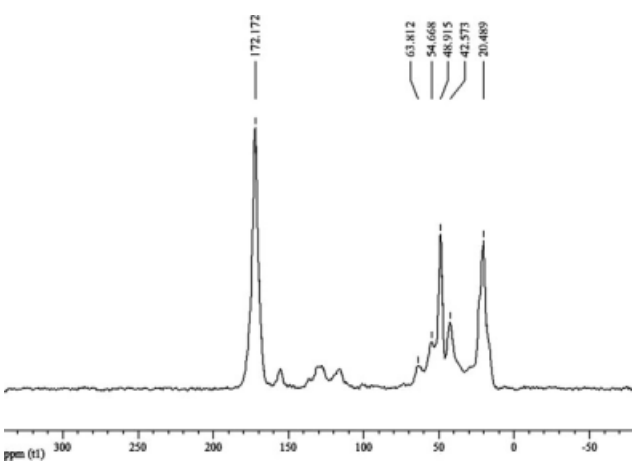

Figure 9 NMR (Nuclear Magnetic Resonance) spectrum of native APSF fiber.

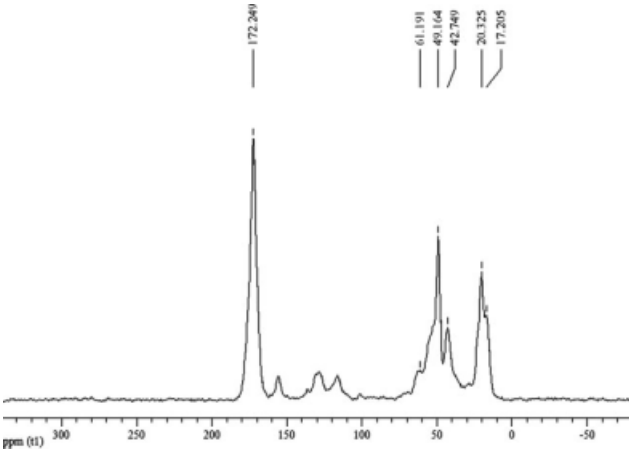

Figure 10 NMR spectrum of regenerated APSF fiber.

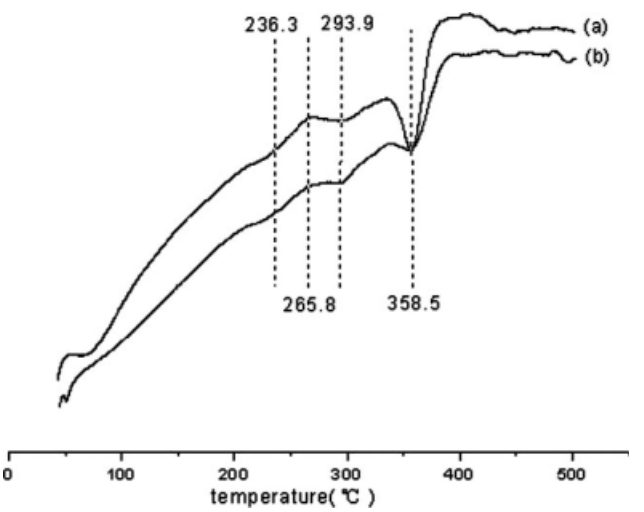

Figure 11 DTA curves of (a) native APSF fibers and (b) regenerated fibers.

the secondary structure of silk fibroin was changed after regeneration. The characteristic resonance of the regenerated fibers was as follows: Ala C_β and C_α at 20.325 and 49.164 ppm, Ser C_β at 61.191 ppm, and Ala C=O at 172.249 ppm (all attributed to the β-sheet structure) and Gly C_α at 42.573 ppm (due to the α-helix conformation). There was little difference with the native fibers with respect to the position of the resonance peaks. However, the peak of Ser C_α at 54.668 due to the β sheet disappeared, and a new peak of Ala C_β at 17.205 due to the random-coil conformation appeared. These changes indicated that the random-coil, α-helix, and β-sheet conformations existed in the regenerated fibers, and this was consistent with the aforementioned analysis.

Thermogravimetric analysis curves

The thermal behavior of *A. pernyi* fibers was studied by means of thermogravimetric measurements. The regenerated and native APSF fibers exhibited similar DTA curve profiles, as shown in Figure 11; an endo–exo transition around 250°C and a minor endothermic peak at 290°C were detected, and these were followed by a prominent endothermic peak at 358°C. The endothermic peak at 236°C was attributed to molecular motion of the α-helix region, and the exothermic peak at 265°C was attributed to crystallization during the heating with the formation of the β-sheet structure from the random-coil conformation.[9,17] Thermal decomposition of APSF fibers with the β-sheet structure occurred at 358°C.[7,9,12] It has been reported that the molecular weights of native APSF and regenerated APSF are 400–450[24] and 200–50 kDa,[25] respectively. The shorter fibroin was tightly aggregated within the crystalline regions after ethanol coagulation. This feature restricted the molecular motion of regenerated filaments induced by heat, and this led to thermal stability similar to that of native silks.

Mechanical properties

The break strength is an important parameter of the mechanical properties of fibers. The break strengths of the native and regenerated APSF fibers were 0.4743 and 0.2476 GPa, respectively.

The break strength of the regenerated fibers was 52.20% of that of the native fibers, possibly because of the decrease in the molecular weight of the regenerated APSF and insufficient wet-spinning draw.

CONCLUSIONS

From this study, these conclusions can be drawn:

1. The molecular weights of the regenerated silk fibroin aqueous solution had a uniform distribution between 60 and 200 kDa.
2. The regenerated APSF had a crystalline structure similar to that of the native fiber, which was mainly a β sheet, but it had more α-helix and random-coil conformations.
3. The regenerated APSF fibers could be spun continually with the HFIP wet-spinning method, and the break strength of the regenerated fibers was 0.2476 GPa, which was only 52.20% of that of the native fibers.

References

1. Minoura, N.; Aiba, S.; Gotoh, Y.; Tsukada, M.; Imai, Y. Biochem Biophys Res Commun 1995, 208, 511.
2. Pierschbacher, M. D.; Ruoslahti, E. Nature 1984, 309, 30.
3. Pierschbacher, M. D.; Ruoslahti, E. Proc Natl Acad Sci USA 1984, 81, 5985.
4. Houseman, B. T.; Mrksich, M. Biomaterials 2001, 22, 943.
5. Shaw, J. T. B.; Smith, S. G. Biochim Biophys Acta 1961, 52, 305.
6. Magoshi, J.; Magoshi, Y.; Nakamura, S. J Appl Polym Sci 1997, 21, 2405.
7. Freddi, G.; Monti, P.; Nagura, M.; Gotoh, Y.; Tsukada, M. J Polym Sci Part B: Polym Phys 1997, 35, 841.
8. Tsukada, M. J Polym Sci Part B: Polym Phys 1986, 24, 457.
9. Li, M. Z.; Tao, W.; Kuga, S.; Nishiyama, Y. Polym Adv Technol 2003, 14, 694.
10. Minoura, N.; Tsukada, M.; Nagura, M. Biomaterials 1990, 11, 430.
11. Tsukada, M.; Freddi, G.; Kasai, N. J Polym Sci Part B: Polym Phys 1998, 36, 2717.
12. Tsukada, M.; Freddi, G.; Gotoh, Y.; Kasai, N. J Polym Sci Part B: Polym Phys 1994, 32, 1407.
13. Kweon, H. Y.; Woo, S. O.; Park, Y. H. J Appl Polym Sci 2001, 81, 2271.
14. Kweon, H. Y.; Um, I. C.; Park, Y. H. Polymer 2000, 41, 7361.
15. Dash, R.; Mukherjee, S.; Kundu, S. C. Int J Biol Macromol 2006, 38, 255.
16. Tsukada, M. J Polym Sci Part B: Polym Phys 1988, 26, 949.
17. Kweon, H. J Appl Polym Sci 2001, 81, 2271.
18. Li, M. Z.; Tao, W.; Lu, S.; Kuga, S. Int J Biol Macromol 2003, 32, 159.
19. Krimm, S.; Bandekar, J. Adv Prot Chem 1986, 38, 181.
20. Tsukada, M.; Freddi, G.; Monti, P.; Bertoluzza, A.; Kasai, N. J Polym Sci Part B: Polym Phys 1995, 33, 1995.
21. Tsukada, M.; Nagura, M.; Ishikawa, H. J Polym Sci Part B: Polym Phys 1987, 25, 1325.
22. Asakura, T.; Nakazawa, Y. Macromol Biosci 2004, 4, 175.
23. Nakazawa, Y.; Nakai, T.; Kameda, T.; Asakura, T. Chem Phys Lett 1999, 311, 362.
24. Tamura, T.; Kubota, T. In Wild Silkmoth; Akai, H.; Wu, Z. S., Eds.; International Society for Wild Silkmoths: Ibaraki, Japan, 1988; p 67.
25. Tsukada, M.; Freddi, G.; Gotoh, Y.; Kasai, N. J Polym Sci Part B: Polym Phys 1994, 32, 1407.